



Article

Disrupting the Conserved Salt Bridge in the Trimerization of Influenza A Nucleoprotein

Jennifer Woodring, Shao-Hung Lu, Larissa Krasnova, Shih-Chi Wang, Jhih-Bin Chen, Chiu-Chun Chou, Yi-Chou Huang, Ting-Jen Cheng, Ying-Ta Wu, Yu-Hou Chen, Jim-Min Fang, Ming-Daw Tsai, and Chi-Huey Wong

J. Med. Chem., **Just Accepted Manuscript** • DOI: 10.1021/acs.jmedchem.9b01244 • Publication Date (Web): 26 Nov 2019

Downloaded from pubs.acs.org on November 27, 2019

Just Accepted

"Just Accepted" manuscripts have been peer-reviewed and accepted for publication. They are posted online prior to technical editing, formatting for publication and author proofing. The American Chemical Society provides "Just Accepted" as a service to the research community to expedite the dissemination of scientific material as soon as possible after acceptance. "Just Accepted" manuscripts appear in full in PDF format accompanied by an HTML abstract. "Just Accepted" manuscripts have been fully peer reviewed, but should not be considered the official version of record. They are citable by the Digital Object Identifier (DOI®). "Just Accepted" is an optional service offered to authors. Therefore, the "Just Accepted" Web site may not include all articles that will be published in the journal. After a manuscript is technically edited and formatted, it will be removed from the "Just Accepted" Web site and published as an ASAP article. Note that technical editing may introduce minor changes to the manuscript text and/or graphics which could affect content, and all legal disclaimers and ethical guidelines that apply to the journal pertain. ACS cannot be held responsible for errors or consequences arising from the use of information contained in these "Just Accepted" manuscripts.

Disrupting the Conserved Salt Bridge in the Trimerization of Influenza A Nucleoprotein

Jennifer L. Woodring,[†] Shao-Hung Lu,^{‡, ||} Larissa Krasnova,[†] Shih-Chi Wang,[‡] Jhih-Bin Chen,^{‡, ||} Chiu-Chun Chou,^{||} Yi-Chou Huang,^{||} Ting-Jen Rachel Cheng,[‡] Ying-Ta Wu,[‡] Yu-Hou Chen,[⊥] Jim-Min Fang,^{‡, ||} Ming-Daw Tsai[⊥] and Chi-Huey Wong.^{†, ‡*}

[†]Department of Chemistry, The Scripps Research Institute, 10550 North Torrey Pines Road, La Jolla, CA 92037, United States.

[‡]Genomics Research Center, Academia Sinica, Taipei 115, Taiwan.

^{||}Department of Chemistry, National Taiwan University, Taipei 106, Taiwan.

[⊥]Institute of Biological Chemistry, Academia Sinica, Taipei 115, Taiwan

JLW and SHL had equal contributions

ABSTRACT: Antiviral drug resistance in influenza infections has been a major threat to public health. In order to develop a broad-spectrum inhibitor of influenza to combat the problem of drug resistance, we previously identified the highly conserved E339...R416 salt bridge of the nucleoprotein trimer as a target, and compound **1** as an inhibitor disrupting the salt bridge with an EC₅₀ = 2.7 μM against influenza A (A/WSN/1933). We have further modified this compound via a structure-based approach and performed an antiviral activity screen to identify compounds **29** and **30** with EC₅₀ values of 110 and 120 nM respectively and without measurable host cell cytotoxicity. Compared to the clinically used neuraminidase inhibitors, these two compounds showed better activity profiles against drug-resistant influenza A strains, as well as influenza B, and improved survival of influenza-infected mice.

■ INTRODUCTION

Influenza viruses infect millions of people every year.¹ Although several antiviral drugs and vaccines targeting specific viral proteins have been developed (*e.g.*, the Neuraminidase inhibitors Zanamivir and Oseltamivir,² and the cap-dependent endonuclease inhibitor baloxavir marboxil³), these drugs are only effective when taken at the onset of infection and their use in the clinic has encountered drug resistance.^{4–6} Vaccines require annual renewal and have limited coverage across various subtypes and mutations.⁷ To tackle the problem of drug resistance in influenza infections, a novel influenza target called the nucleoprotein (NP) was reported.^{8–12} This protein encapsidates the viral genome, including RNA and RNA polymerase, as well as plays an essential role in viral replication. It accumulates in the nucleus during early infection, distributes in

the cytoplasm during viral assembly and maturation, and has a tail-loop region that helps the NP form trimers through the highly conserved E339...R416 salt bridge (**Figure 1A**).^{13–16} Through high-throughput campaigns performed by us and others, some small molecules were found to inhibit the influenza RNA polymerase activity by promoting aggregation of NP¹⁷ or by blocking the transport of NP to the nucleus.¹⁸ However, resistance to the inhibitor of RNA polymerase emerges quickly so targeting the highly conserved salt bridge involved in NP trimerization would be advantageous. The confirmed hits from our initial primary screening of anti-influenza compounds were selected for further investigation. Through secondary assays and virtual screening using pharmacophore mapping, compound **1** was identified as an effective inhibitor of the E339...R416 salt bridge in the protein-protein interaction of influenza NP trimerization.¹⁹ It was

hypothesized that compound **1** obstructs the guanidino group of R416 to interact with the carboxyl group of E339; thus, disrupting the salt bridge to prevent NP from trimerization (**Figure 1B**, see **Figure S1** for the PDB model). Compound **1** (**Figure 2A**) has a modest antiviral potency with an EC_{50} of 2.7 μ M yet exhibits MDCK toxicity.¹⁹ In order to further improve the potency and selectivity, we describe here the identification of the key pharmacophore associated with the antiviral activity of compound **1** and its optimization via structure- and activity-based drug discovery approaches to identify new lead compounds. Given the challenges in developing effective inhibitors against protein-protein interactions and the comprehensive set of inhibitors identified in this study, we believe this work represents a new direction toward the solution of drug resistance in influenza infection.

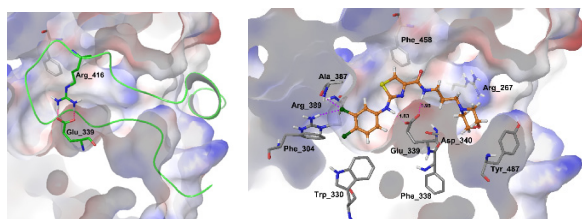


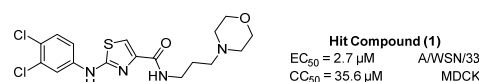
Figure 1. (A) Molecular modeling of the E339...R416 salt bridge, which is essential for NP trimerization, in the protein-protein interaction within the tail-loop region (shown as a green ribbon), and (B) the complex that compound **1** is docked into the tail-loop binding pocket.

RESULTS AND DISCUSSION

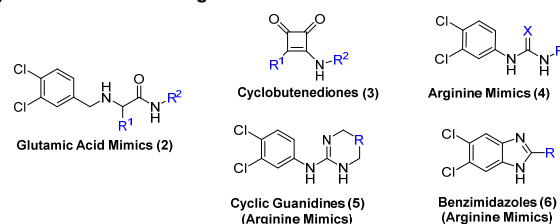
Our approach to the structure-activity-relationship (SAR) study of compound **1** focused on two design strategies: (1) structure-based design, where the arginine and glutamic acid mimics were incorporated into the compound to specifically interact with the E339 or R416 residues in the salt bridge formed during influenza NP trimerization, and (2) activity-based screening using the virus-induced cytopathic effects, where each functional group or motif of the compound was individually modified and the antiviral activity of the analogue was determined directly through measuring the cell death induced by infection of influenza A/WSN/1933 (H1N1) virus. For each of these design strategies, several libraries were pursued, as shown in **Figure**

2B and **2C**, and their syntheses are outlined in **Scheme 1**, as well as in the Supporting Information. Of the 9 total libraries, only the compounds with cyclobutenedione (**3**), cyclic guanidine (**5**), aniline (**7**), amide (**8**), and propyl-morpholine substitutions (**10**) had a wide range of activities (**Table S1-S11**, and **Figure S1**). The thiazole replacements (**9**) and arginine mimics (**4**) only gave 1 or 2 compounds, respectively, with any measurable potency. Neither the glutamic acid set (**2**) nor the benzimidazole series (**6**) gave any active compounds. In general, modifications made to the secondary amine of the aniline, thiazole ring, amide bond, or propyl chain did not produce any significant increase in activity, as compared to compound **1**.

(A) Screening Hit



(B) Structure-Based Design



(C) Activity-based Screening Using Virus-induced Cytopathic Effects

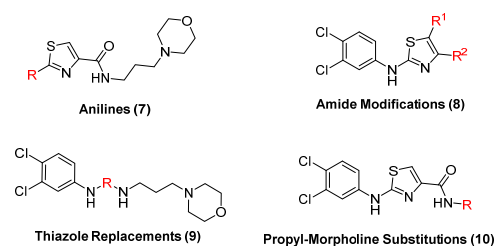


Figure 2. (A) Structure and activity of the hit compound **1** identified by high-throughput screening, (B) the 5 libraries pursued for the structure-based approach in which the replacements acted as arginine or glutamic acid mimics to target the E339...R416 salt bridge, and (C) the 4 libraries pursued under the activity-based screening approach in which each moiety of compound **1** was modified

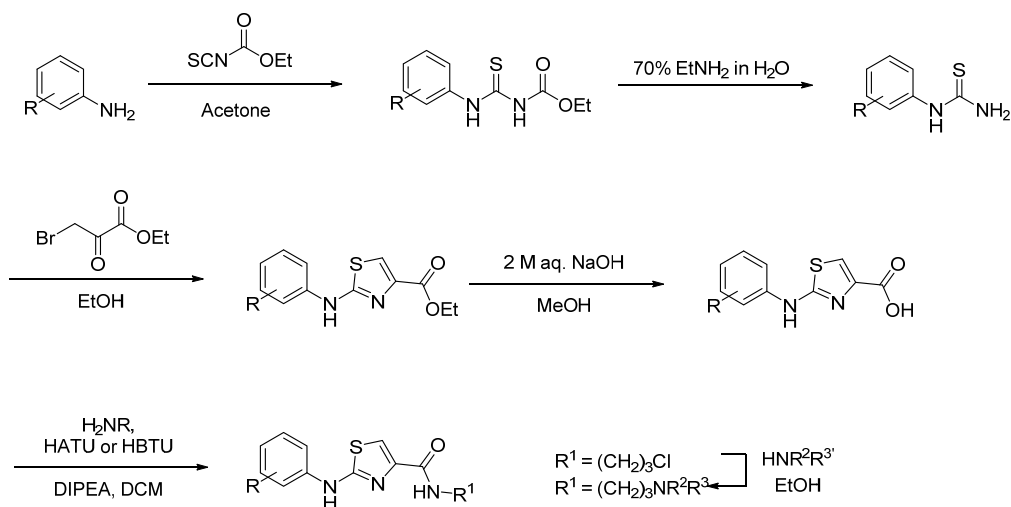
and the analogs were analyzed for their impact on cell death induced by infection of influenza virus.

Overall, the aniline (**7**) and propyl-morpholine substitutions (**10**) libraries generated more active compounds than any other sets and were the only series to have compounds with sub-micromolar potencies

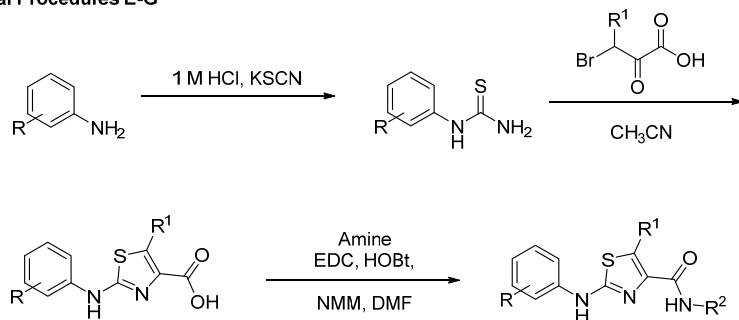
(see **Table S1–S11**). From these libraries, we identified the best aniline ($EC_{50} < 5 \mu M$) and propyl-morpholine ($EC_{50} < 1 \mu M$) replacements, which were used to design cross-over compounds combining these best moieties in order to further improve the potency.

Scheme 1. General synthetic schemes.

General Procedures A-D



General Procedures E-G



General Procedures H-I

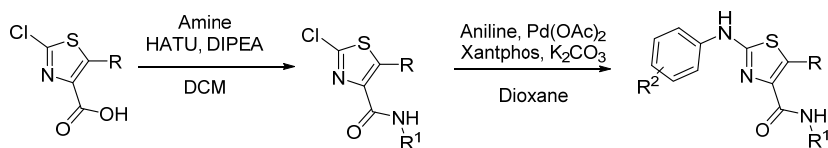
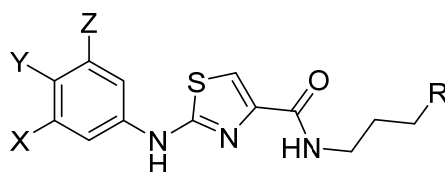


Table 1. Potency and host cell cytotoxicity of cross-over compounds containing motifs from the best aniline ($EC_{50} = <5 \mu M$) and best morpholine replacement ($EC_{50} = <1 \mu M$) libraries.



Compound	X	Y	Z	R	EC_{50} (μM)	CC_{50} (μM)
1	Cl	Cl	H	Morpholine	2.7	35.6
11	Cl	Cl	H	OiPr	0.7	100
12	Cl	Cl	H	OEt	0.2	>100
13	Cl	Cl	Cl	Morpholine	1.5	41
14	Cl	Cl	Cl	OiPr	0.6	>100
15	Cl	Cl	Cl	OEt	0.4	>100
16	H	Cl	H	Morpholine	3.1	>100
17	H	Cl	H	OiPr	1.2	>100
18	H	Cl	H	OEt	1.3	>100
19	CH ₃	Cl	H	Morpholine	3.7	47
20	CH ₃	Cl	H	OiPr	1.2	>100
21	CH ₃	Cl	H	OEt	1.0	52
22	CH ₃	Cl	CH ₃	Morpholine	3.1	45.7
23	CH ₃	Cl	CH ₃	OiPr	1.3	>100
24	CH ₃	Cl	CH ₃	OEt	2.3	>100
25	F	Cl	H	Morpholine	3.2	45
26	F	Cl	H	OiPr	0.5	>100
27	F	Cl	H	OEt	0.6	>100
28	F	Cl	F	Morpholine	0.8	52
29	F	Cl	F	OiPr	0.11	>100
30	F	Cl	F	OEt	0.12	>100

To explore the proper carbon distance for the linker of these two groups, we synthesized five compounds bearing hydroxyl group with different distance chain length (compounds **S167-S171** in **Table S10**) and showed that only 3-carbon distance compound (the compound **S168**) had the measurable activity. Furthermore, the linker tailing with oxygen atom improved the binding affinity (see **Table S10**, compounds **S172-S177**). In every case, replacing the morpholine (**R**) with an ether group improved the potency. Both outcomes were aligned with the observation from the molecular model (Figure **1B**), in which the side chain guanidino group of Arg267 and the backbone alpha-amino group of Asp340 create an environment preferring electronegative hydrogen-bonding acceptor atoms at the linker end; the cleft formed by Phe338 and Tyr487 suggesting a hydrophobic tailing group after the 3-carbon linker. Therefore, a series of ethers were synthesized in the study of propyl-morpholine substitutions. Among the sub-micromolar compounds, the ethers in the propyl-morpholine substitutions, such as OiPr and OEt groups, were in general obtaining better affinity than compounds with morpholine, yet exhibited less MDCK host cell cytotoxicity (**Table 1** and **Table S10**). Since the ether replacements resulted in compounds with both higher potency and selectivity, the ethers were preferred over the amines and solely used in the cross-over compound series.

The results for the cross-over compounds can be found in **Table 1**. The chlorine moiety at the 3-position of the aniline (X) could be substituted with a hydrogen, fluorine, or methyl with little effect on the potency. Any changes to the chlorine at the 4-position (Y) were not tolerated in the assay. If symmetry was created by adding a functional group at the 5-position of the aniline ring (Z), it maintained or improved the potency when compared to the corresponding aniline without symmetry (as seen in **1** vs. **13**, **19** vs. **22**, and **25** vs. **28**). In every case, replacing the morpholine (**R**) with an isopropyl or ethyl ether improved the potency. There are two reasons why replacing the morpholine (**R**) with an isopropyl or ethyl ether would improve the potency. However, for the ether derivatives, only the anilines with a halogen (F, Cl) and not an aliphatic group (H, CH₃) at the 3-position, exhibited sub-micromolar potencies. Our modeling also indicated that halide anilines are better than other aryl substitutions

(**Table S7** and Figure **S2**). Especially, the para-chlorine, but not the meta-chlorine, on the aniline ring of Compound **29** and **30** could increase the binding by forming halogen-bonding interactions with Arg389 and Ala387; the two fluorine atoms by forming weak hydrogen bonding interactions with Phe304, Trp330, and Ala387 (see Figure **S2**). It is noted that the potencies for the aliphatic anilines improved slightly by a factor of 2-3 when incorporating the ether group (e.g. **16** vs. **17** and **18**), whereas the potencies for the halogen anilines improved the activity more greatly compared to the morpholines (e.g. 2.5-fold for **14** and 3.8-fold for **15** compared to **13**, 7.3-fold for **29** and 6.7-fold for **30** compared to **28**).

Because of their high potency and great selectivity profile, both compounds **29** and **30** were selected for additional studies. These compounds, along with compound **1** and three neuraminidase inhibitors (Oseltamivir, Zanamivir, and Peramivir), were screened against a panel of 9 influenza strains (**Table S12**). The comparison of the anti-influenza activities (pEC₅₀ values) for compound **1**, compound **29**, and compound **30** to each of the neuraminidase inhibitors is displayed in the heat map in **Figure 3**. In most cases, compound **1** did not perform as well as the other analogs across the influenza virus strains, but the two new compounds **29** and **30** had better potencies than neuraminidase inhibitors for almost all tested H1N1 influenza virus strains, one H5N1 recombinant virus and one influenza B strain virus (denoted by darker shades of blue).

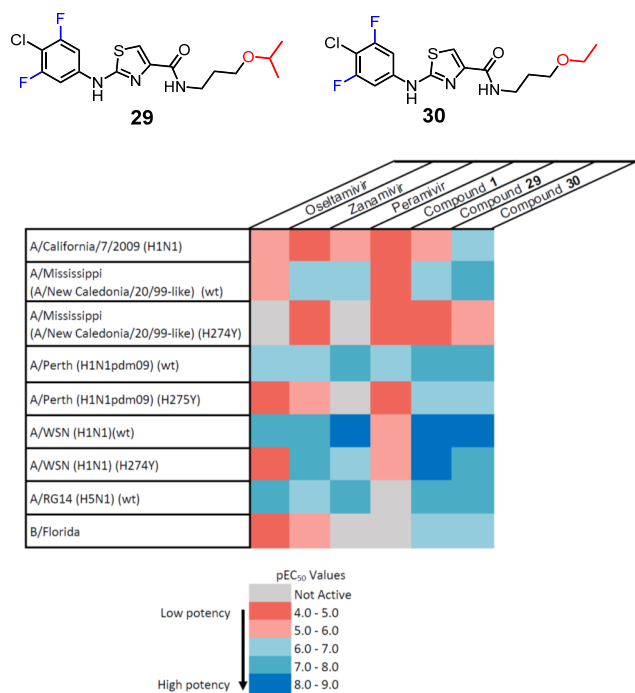
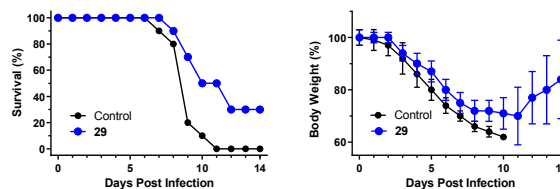


Figure 3. Heat map detailing the pEC₅₀ values for neuraminidase inhibitors Oseltamivir, Zanamivir, and Peramivir, as well as compound **1**, compound **29**, and compound **30**. Red color denotes low pEC₅₀ values with potencies in the micromolar range, while the blue color denotes higher pEC₅₀ values with potencies in the nanomolar range. Gray color denotes no measurable activity for that influenza strain.

In addition to cell-based assays using a panel of influenza virus strains, compounds **29** and **30** were also tested in an animal virus challenge model to determine their *in vivo* efficacy. This virus challenge model has been successfully used to evaluate the activities of oseltamivir, zanamivir, and their analogues.^{20,21,22} The Balb/c mice were subjected to two times the lethal dose (2x LD₅₀) of the influenza A/WSN/1933 (H1N1) virus. Due to poor aqueous solubility, compound **29** was screened as a disulfate salt and compound **30** as a dimesylate salt. The compounds were dosed intraperitoneally for 5 days at concentrations of 20 mg/kg/day. The resulting survival rates post infection are shown in **Figure 4**. The survival rate was extended to 30% for compound **29** and to 70% for compound **30**. Also, the body weight of the treated mice dropped upon virus

challenges and recovered gradually after 10 days post virus-infection.

(A)



(B)

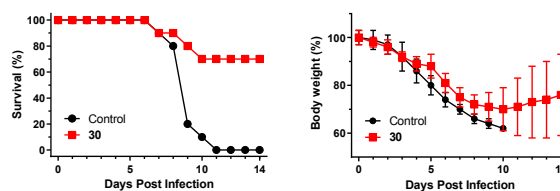


Figure 4. Representative virus challenge studies at 2x LD₅₀ A/WSN/1933 (H1N1) for (A) compound **29** as a disulfate salt, and (B) compound **30** as a dimesylate salt, both with dosing at 20 mg/kg/day for 5 days. Control mice received phosphate-buffered saline containing 40% polyethylene glycol 400 on the same schedule.

Docking of compound **29** in the E339...R416 binding site (**Figure 5**) gives a more detailed analysis of how this compound disrupts the protein-protein interaction. The carboxyl group of the Glu339 residue, which forms the salt bridge with the tail-loop Arg416 residue, exerts at least two hydrogen bonding interactions with both secondary amines of this compound. As for halogen-bonding interactions, the chlorine on the aniline non-covalently binds with the Arg389 and Ala387 residues. In compound **29**, one fluorine interacts with the Arg389 residues (with longer distances compared to the interaction with chlorine), while the other fluorine interacts with the Phe304 and Trp330 residues (**Figure S2**). Additionally, the aromaticity of the thiazole ring could undergo π - π stacking with Phe458, and the new ethyl ether is oriented towards the hydrophobic cleft formed by Phe338 and Tyr487.

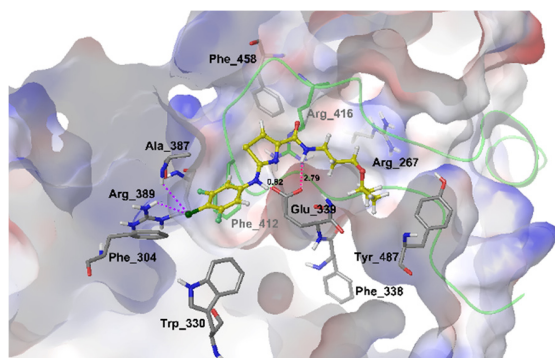


Figure 5. Modeling of compound **29** involved in the disruption of the highly conserved E339...R416 salt bridge in the protein-protein interaction during NP trimerization (tail-loop shown as green ribbon). The influenza nucleoprotein (PDB code 2IQH) was used. The 3D model of the binding site shows the halogen-bonding interactions between the fluorine and chlorine atoms of the aniline ring with Phe304, Trp330, Ala387 and Arg389 residues, the hydrogen-bond interactions between the Glu339 residue and the secondary amines of compound **29**, and the hydrophobic interaction between the isopropyl ether portion of the molecule and the well-defined hydrophobic cleft.

Further analysis based on NP mass distribution by analytical ultracentrifuge showed that binding of compounds **29** and **30** causes inhibition of NP oligomerization and trimerization, indicating the same mode of action as compound **1** (Figure S5). In addition, both compounds **29** and **30** are more effective than compound **1** on disruption of NP-NP interaction (Figure S5).

CONCLUSION

In conclusion, the E339...R416 salt bridge of the nucleoprotein is a novel drug target for the development of inhibitors against the influenza A virus. From the SAR study of analog **1**, we developed compounds **29** and **30** with a 23-fold enhancement in potency and no measurable host cell cytotoxicity effect. These two novel compounds were also more active than three commercially developed neuraminidase inhibitors against a set of mutated influenza strains and prolonged the survival rate of infected mice in the animal challenge studies. Our results

suggest that compounds **29** and **30** have a significant potential for further development into a new class of antiviral therapeutics targeting the highly conserved E339...R416 salt bridge in the trimerization of the influenza nucleoprotein.

EXPERIMENTAL SECTION

General Methods for Compound Synthesis. Reagents were purchased from Alfa Aesar, Acros, Chem Impex, Combi-Blocks, Fisher, Oakwood, Sigma-Aldrich, Strem, or TCI chemical companies and used as received. Solvents were purchased from Acros, Fisher, Sigma-Aldrich, or VWR chemical companies and used as received (no extra drying, distillation or special handling practices were employed). Thin layer chromatography (TLC) analyses were performed on EMD 250 μ m Silica Gel 60 F254 plates and visualized by short wave UV light ($\lambda_{\text{max}} = 254$ nm), staining only when indicated for individual compounds. Microwave reactions were performed on a Biotage Initiator+ system. Flash column chromatography was performed using a Biotage Isolera™ One flash system with silica gel cartridges: KP-Sil (50 μ m irregular silica), HP-Sphere™ (25 micron spherical silica) and KP-C18-HS. Purest fractions from chromatography provided the percent yields reported and any impure fractions were discarded. These analogs were determined to be >95% purity by LCMS and NMR analyses prior to biological testing.

Compound Analysis. Optical rotations were obtained on a Perkin Elmer 341 Polarimeter with a sodium D line ($\lambda = 589$ nm) light source and a cylindrical glass cell with path length of 1.0 dm. Melting points were determined on a Barnstead Electrothermal 1A9300 apparatus. All newly synthesized compounds were deemed >95% pure by LCMS and NMR analysis. For MS analysis, low-resolution LCMS analysis was performed using an Agilent 1100 series reverse-phase LC/MSD and Agilent Zorbax 5 μ m C8 4.6 x 50 mm column, with an Agilent G1956B single-quadrupole mass spectrometer (electrospray ionization positive mode). Mobile phases consisted of water/0.1% formic acid and acetonitrile/0.1% formic acid. Gradient started out at 95% aqueous and ramped to 95% organic in 7 minutes. Stop time was set to 10 min, with a four minute post time. High-resolution LCMS analysis

was performed using an Agilent G1969A ESI-TOF (electrospray ionization – time of flight) mass spectrometer with a capillary voltage of 4000V and 200 $\mu\text{L}/\text{min}$ flow rate. Data also acquired in positive mode. Samples were directly infused, with the mobile phase set to 90:10 (acetonitrile/0.1% formic acid: water 0.1% formic acid). NMR spectra were recorded on Bruker DRX-500, DRX-600 and AV-400 instruments. The chemical shifts (δ) are expressed in parts per million (ppm) relative to residual signals of $(\text{CD}_3)_2\text{CO}$ (^1H NMR = 2.05 ppm, ^{13}C NMR 29.8, 206.3 ppm), CDCl_3 (^1H NMR = 7.26 ppm, ^{13}C NMR = 77.2 ppm) CD_2Cl_2 (^1H NMR = 5.32 ppm, ^{13}C NMR 53.8 ppm), $(\text{CD}_3)_2\text{NCDO}$ (^1H NMR = 2.75, 2.92, 8.03 ppm, ^{13}C NMR 29.8, 34.9, 163.2 ppm), $(\text{CD}_3)_2\text{SO}$ (^1H NMR = 2.50 ppm, ^{13}C NMR = 39.5 ppm), and CD_3OD (^1H NMR = 3.31 ppm, ^{13}C NMR 49.0 ppm) as internal standards. Spectra were analyzed using ACD Labs and MestraNova NMR processing software.

Synthesis and Characterization of Compounds 1, 11 – 30

General procedure A – Synthesis of ethyl 3-thioureidocarboxylates (Scheme 1).²³ The respective aniline (1.0 equiv) was dissolved in anhydrous acetone (0.15 M) and then ethoxycarbonyl isothiocyanate (1.1 equiv) was added. The mixture was heated at 40 $^\circ\text{C}$ for 20 minutes and then room temperature for 12 hours. The reaction mixture was concentrated under reduced pressure until dry. Then 10 mL of anhydrous cyclohexane was added and the mixture sonicated. The precipitate was collected by vacuum filtration to obtain the product.

General procedure B – Synthesis of thioureas from thioureidocarboxylates (Scheme 1). The respective thioureidocarboxylate (1.0 equiv) was dissolved in 10.0 equivalents of a 70% solution of ethylamine in water. The mixture stirred at room temperature for 12 hours, diluted with methanol, and concentrated under reduced pressure until dry. Then 10 mL of anhydrous cyclohexane was added and the mixture sonicated. The precipitate was collected by vacuum filtration to obtain the product. Alternatively, 50.0 equivalents of 28-30% ammonium hydroxide can be used in lieu of aqueous ethylamine. However, the total reaction time for ammonium hydroxide was 2-3 days.

General procedure C – Synthesis of 2-(amino)thiazole-4-carboxylic acids via ester

synthesis (Scheme 1). The respective thiourea (1.0 equiv) was dissolved in ethanol (0.47 M). To this solution was added 80% ethyl bromopyruvate (1.0 equiv) and the reaction proceeded in the microwave for 30 minutes at 150 $^\circ\text{C}$. The reaction mixture was concentrated under reduced pressure until dry. To the crude ester compound was added a 1:1 solution of MeOH and 2M aqueous NaOH (0.2 M) and the mixture stirred at room temperature for 12 hours. The mixture was neutralized to a pH of 5 with 1 M HCl and the resulting precipitate was collected by vacuum filtration to obtain the desired product.

General procedure D – HATU amide couplings (Scheme 1). In a flask, 2-((3,4-dichlorophenyl)amino)thiazole-4-carboxylic acid or a similar carboxylic acid (1.0 equiv) and HATU (1.0 equiv) were suspended in dichloromethane (0.10 M). While stirring, DIPEA (2.0 equiv), and the respective amine (1.0 equiv) were added to the suspension. The mixture was stirred at room temperature for 12 hours, diluted with water, and the organic layer was extracted 3 times with dichloromethane. The combined organic layers were evaporated under reduced pressure and purified by reversed-phase chromatography (water/acetonitrile) to obtain the final products. Any variances are denoted with each compound.

General procedure E – Synthesis of thioureas from anilines (Scheme 1). To a solution of aniline (1.0 equiv) in 1M HCl (0.4 M) was added potassium thiocyanate (4.6 equiv) under argon at room temperature. The mixture was stirred at 110 $^\circ\text{C}$ for 15 hours. The precipitate was filtered and washed with cold water to afford the desired thiourea, which was used without further purification.

General procedure F – Synthesis of 2-(amino)thiazole-4-carboxylic acids from thioureas (Scheme 1). To a solution of the thiourea (1 equiv.) in CH_3CN (0.3 M) was added bromopyruvic acid (1 equiv.) under argon at room temperature. The mixture was stirred at 80 $^\circ\text{C}$ for 18 hours. The precipitate was filtered and washed with cold CH_3CN to afford the desired intermediate which was used without further purification.

General procedure G - HOBt couplings (Scheme 1). To a solution of the carboxylic acid (1.0 equiv) in DMF and *N*-methylmorpholine (0.05 M, 1:0.04 DMF:*N*-methylmorpholine) were added 1-ethyl-3-(3-dimethylaminopropyl)carbodiimide (4.4 equiv) and hydroxybenzotriazole (4.4 equiv) under argon at room temperature. The mixture was stirred at room temperature for 10 minutes then amine (1.0 equiv) was added slowly. The mixture was stirred at room temperature for 10 hours. After evaporation in vacuo to remove DMF and *N*-methylmorpholine, the reaction mixture was acidified with 1 M HCl and extracted with water and CH₂Cl₂. The aqueous layer was basified with 1 M NaOH and extracted with CH₂Cl₂. The organic layer was then separated, dried over anhydrous magnesium sulfate. After concentrated under reduced pressure, the residue was purified by SiO₂ column chromatography to afford the amide compound.

General procedure H - Amide coupling reactions with 2-chlorothiazoles (Scheme 1). In a flask, 2-chlorothiazole-4-carboxylic acid or similar 2-chlorothiazole (1.0 equiv) and HATU (1.0 equiv) were suspended in dichloromethane (0.12 M). To this mixture was added DIPEA (2.0 equiv) and then the amine (1.0 equiv). The mixture stirred at room temperature for 12 hours. The reaction mixture was diluted with water and extracted with dichloromethane three times. The organic layers were combined and concentrated under reduced pressure. The product was purified by reversed-phase chromatography (water/acetonitrile).

General procedure I - Buchwald coupling reactions (Scheme 1).²⁴ For each reaction, a mixture of 2-chloro-*N*-(3-morpholinopropyl)thiazole-4-carboxamide or similar 2-chlorothiazole (1.0 equiv), palladium (II) acetate (0.1 equiv), xantphos (0.2 equiv), potassium carbonate (3.0 equiv), the respective aniline (1.2 equiv), and anhydrous 1,4-dioxane (0.09 M) was refluxed at 105 °C for 12 hours. Precipitates were filtered off via vacuum filtration and discarded. The remaining filtrate was concentrated under reduced pressure and purified by reversed-phase chromatography (water/acetonitrile). If aniline starting material remained after the column, the crude product was suspended in cyclohexane, sonicated, and the precipitate collected by

vacuum filtration to obtain the final desired product.

Ethyl 3-(3,4-dichlorophenyl)thioureidocarboxylate. Scheme 1, general procedure A, using 3,4-dichloroaniline. White solid, 98% yield (226.3 mg). *R_f* = 0.74 (100% DCM). m.p. 125.6-134.8 °C. ¹H NMR (600 MHz, (CD₃)₂SO) δ ppm 11.54 (s, 1 H), 11.39 (s, 1 H), 8.01 (d, *J* = 1.5 Hz, 1 H), 7.64 (d, *J* = 8.7 Hz, 1 H), 7.55 (dd, *J* = 8.5 Hz, 1.8 Hz, 1 H), 4.21 (q, *J* = 6.9 Hz, 2 H), 1.26 (t, *J* = 7.1 Hz, 3 H). ¹³C NMR (151 MHz, (CD₃)₂SO) δ ppm 179.1, 153.3, 138.2, 130.6, 128.1, 126.4, 125.1, 62.1, 14.1. HRMS (ESI-TOF) calcd for C₁₀H₁₁Cl₂N₂O₂S: 292.9913, found 292.9912 [M+H]⁺.

Ethyl 3-(3,4,5-trichlorophenyl)thioureidocarboxylate. Scheme 1, general procedure A, using 3,4,5-dichloroaniline. Off-white solid, 87% yield (328.9 mg). *R_f* = 0.81 (100% DCM). m.p. 141.4-145.5 °C. ¹H NMR (600 MHz, (CD₃)₂SO) δ ppm 11.55 (s, 1 H), 11.48 (s, 1 H), 7.97 (s, 2 H), 4.22 (q, *J* = 7.0 Hz, 2 H), 1.26 (t, *J* = 7.1 Hz, 3 H). ¹³C NMR (151 MHz, (CD₃)₂SO) δ ppm 179.3, 153.2, 138.3, 132.3, 126.8, 125.5, 62.2, 14.1. HRMS (ESI-TOF) calcd for C₁₀H₁₀Cl₃N₂O₂S: 326.9523, found 326.9526 [M+H]⁺.

Ethyl 3-(4-chlorophenyl)thioureidocarboxylate. Scheme 1, general procedure A, using 4-chloroaniline. Pale yellow solid, 91% yield (423.2 mg). *R_f* = 0.70 (100% DCM). m.p. 121.9-129.7 °C. ¹H NMR (600 MHz, (CD₃)₂SO) δ ppm 11.51 (s, 1 H), 11.30 (s, 1 H), 7.62 (d, *J* = 8.5 Hz, 2 H), 7.44 (d, *J* = 8.5 Hz, 2 H), 4.21 (q, *J* = 7.1 Hz, 2 H), 1.26 (t, *J* = 6.9 Hz, 3 H). ¹³C NMR (151 MHz, (CD₃)₂SO) δ ppm 178.9, 153.5, 137.1, 130.1, 128.5, 126.4, 62.1, 14.1. HRMS (ESI-TOF) calcd for C₁₀H₁₂ClN₂O₂S: 259.0302, found 259.0303 [M+H]⁺.

Ethyl 3-(4-chloro-3-fluorophenyl)thioureidocarboxylate. Scheme 1, general procedure A, using 4-chloro-3-fluoroaniline. Pale yellow solid, 99% yield (485.0 mg). *R_f* = 0.69 (100% DCM). m.p. 167.4-168.9 °C. ¹H NMR (600 MHz, (CD₃)₂SO) δ ppm 11.59 (s, 1 H), 11.39 (s, 1 H), 7.90 (dd, *J* = 11.1, 2.3 Hz, 1 H), 7.60 (t, *J* = 8.6 Hz, 1 H), 7.43 (m, 1 H), 4.22 (q, *J* = 7.2 Hz, 2 H), 1.26 (t, *J* = 7.1 Hz, 3 H). ¹³C NMR (151 MHz, (CD₃)₂SO) δ ppm 178.9, 156.5 (d, *J* = 244.3 Hz), 153.4, 138.6 (d, *J* = 9.9 Hz), 130.2, 121.7 (d, *J* = 3.3 Hz), 116.3 (d, *J* = 17.6 Hz), 112.9 (d, *J* =

25.3 Hz), 62.2, 14.1. HRMS (ESI-TOF) calcd for $C_{10}H_{11}ClFN_2O_2S$: 277.0208, found 277.0209 $[M+H]^+$.

Ethyl 3-(4-chloro-3,5-difluorophenyl)thioureido-carboxylate. **Scheme 1**, general procedure A, using 4-chloro-3,5-difluoroaniline. Brown solid, 89% yield (421.1 mg). R_f = 0.76 (100% DCM). m.p. 148.9-156.3 °C. 1H NMR (600 MHz, $(CD_3)_2SO$) δ ppm 11.65 (s, 1 H), 11.48 (br. s, 1 H), 7.76 (m, 2 H), 4.22 (q, J = 7.2 Hz, 2 H), 1.26 (t, J = 7.2 Hz, 3 H). ^{13}C NMR (151 MHz, $(CD_3)_2SO$) δ ppm 179.0, 157.4 (dd, J = 247.6, 5.5), 153.3, 138.5 (t, J = 13.2 Hz), 108.7 (m), 105.0 (t, J = 20.9 Hz), 62.2, 14.1. HRMS (ESI-TOF) calcd for $C_{10}H_{10}ClF_2N_2O_2S$: 295.0114, found 295.0115 $[M+H]^+$.

1-(3,4-Dichlorophenyl)thiourea. **Scheme 1**, general procedure B, using ethyl 3-(3,4-dichlorophenyl)thioureidocarboxylate. Off-white solid, 96% yield (77.8 mg). R_f = 0.48 (5% MeOH in DCM). m.p. 214.4-218.3 °C. 1H NMR (600 MHz, $(CD_3)_2SO$) δ ppm 9.87 (s, 1 H), 7.91 (d, J = 2.3 Hz, 1 H), 7.99 (br. s, 1 H), 7.54 (d, J = 8.7 Hz, 1 H), 7.38 (dd, J = 8.7, 2.6 Hz, 1 H), 7.39 (br. s, 1 H). ^{13}C NMR (151 MHz, $(CD_3)_2SO$) δ ppm 181.3, 139.5, 130.6, 130.3, 125.7, 123.9, 122.7. HRMS (ESI-TOF) calcd for $C_7H_7Cl_2N_2S$: 220.9701, found 220.9702 $[M+H]^+$.

1-(3,4,5-Trichlorophenyl)thiourea. **Scheme 1**, general procedure B, using ethyl 3-(3,4,5-trichlorophenyl)thioureidocarboxylate. Pale yellow solid, 99% yield (232.1 mg). R_f = 0.58 (5% MeOH in DCM). m.p. 179.5-181.5 °C. 1H NMR (600 MHz, $(CD_3)_2SO$) δ ppm 10.00 (s, 1 H), 8.23 (br. s, 1 H), 7.83 (s, 2 H), 7.55 (br. s, 1 H). ^{13}C NMR (151 MHz, $(CD_3)_2SO$) δ ppm 181.3, 139.7, 132.3, 124.0, 122.4. HRMS (ESI-TOF) calcd for $C_7H_6Cl_3N_2S$: 254.9312, found 254.9315 $[M+H]^+$.

1-(4-Chlorophenyl)thiourea. **Scheme 1**, general procedure B, using ethyl 3-(4-chlorophenyl)thioureidocarboxylate. Pale yellow solid, 98% yield (665.4 mg). R_f = 0.55 (5% MeOH in DCM). m.p. 174.7-178.9 °C. 1H NMR (600 MHz, $(CD_3)_2SO$) δ ppm 9.83 (s, 1 H), 7.59 (m, 2 H), 7.49 (m, 2 H), 7.37 (m, 2 H). ^{13}C NMR (151 MHz, $(CD_3)_2SO$) δ ppm 181.2, 138.3, 128.4, 128.0, 124.5. HRMS (ESI-TOF) calcd for $C_7H_8ClN_2S$: 187.0091, found 187.0092 $[M+H]^+$.

1-(4-Chloro-3-fluorophenyl)thiourea. **Scheme 1**, general procedure B, using ethyl 3-(4-chloro-3-

fluorophenyl)thioureidocarboxylate. Pale yellow solid, 96% yield (653.3 mg). R_f = 0.42 (5% MeOH in DCM). m.p. 164.9-181.7 °C. 1H NMR (600 MHz, $(CD_3)_2SO$) δ ppm 10.04 (s, 1 H), 7.79 (br. s, 2 H), 7.82 (dd, J = 11.7, 2.2 Hz, 1 H), 7.48 (t, J = 8.7 Hz, 1 H), 7.23 (ddd, J = 8.7, 2.3, 1.0 Hz, 1 H). ^{13}C NMR (151 MHz, $(CD_3)_2SO$) δ ppm 181.2, 156.7 (d, J = 244.3 Hz), 140.1 (d, J = 8.8 Hz), 130.3, 119.4 (d, J = 3.3 Hz), 114.0 (d, J = 17.6 Hz), 110.7 (d, J = 25.3 Hz). HRMS (ESI-TOF) calcd for $C_7H_7ClFN_2S$: 204.9997, found 204.9997 $[M+H]^+$.

1-(4-Chloro-3,5-difluorophenyl)thiourea. **Scheme 1**, general procedure B, using ethyl 3-(4-chloro-3,5-difluorophenyl)thioureidocarboxylate. Brown solid, 97% yield (279.0 mg). R_f = 0.51 (5% MeOH in DCM). m.p. 159.9-164.4 °C. 1H NMR (600 MHz, $(CD_3)_2SO$) δ ppm 10.09 (s, 1 H), 8.13 (br. s, 1 H), 7.56 (m, 2 H), 7.48 (br. s, 1 H). ^{13}C NMR (151 MHz, $(CD_3)_2SO$) δ ppm 181.2, 157.5 (dd, J = 244.3, 5.5 Hz), 140.1 (t, J = 13.2 Hz), 105.8 (m), 102.1 (t, J = 22.0 Hz). HRMS (ESI-TOF) calcd for $C_7H_6ClF_2N_2S$: 222.9903, found 222.9904 $[M+H]^+$.

2-((3,4-Dichlorophenyl)amino)thiazole-4-carboxylic acid. **Scheme 1**, general procedure C, using 1-(3,4-dichlorophenyl)thiourea. Off-white solid, 97% yield (3.1539 g). Decomposes at 288.9 °C. 1H NMR (500 MHz, $(CD_3)_2SO$) δ ppm 10.76 (br. s, 1 H), 8.16 (m, 1 H), 7.79 (s, 1 H), 7.58 (m, 2 H). ^{13}C NMR (151 MHz, $(CD_3)_2SO$) δ ppm 162.1, 162.1, 143.4, 140.8, 131.1, 130.7, 122.3, 119.1, 117.8, 117.0. HRMS (ESI-TOF) calcd for $C_{10}H_7Cl_2N_2O_2S$: 288.9600, found 288.9602 $[M+H]^+$.

2-((3,4,5-Trichlorophenyl)amino)thiazole-4-carboxylic acid. **Scheme 1**, general procedure C, using 1-(3,4,5-trichlorophenyl)thiourea. Light brown solid, 99% yield (585.5 mg). Decomposes at 271.8 °C. 1H NMR (600 MHz, $(CD_3)_2SO$) δ ppm 12.82 (br. s, 1 H), 11.26 (s, 1 H), 8.02 (s, 2 H), 7.82 (s, 1 H). ^{13}C NMR (151 MHz, $(CD_3)_2SO$) δ ppm 161.9, 161.8, 143.3, 140.7, 132.9, 120.7, 119.8, 116.8. HRMS (ESI-TOF) calcd for $C_{10}H_6Cl_3N_2O_2S$: 322.9210, found 322.9211 $[M+H]^+$.

Scheme 1, general procedure E and F, using 3,4,5-trichloroaniline. White solid, 81% yield (1.3 g).

2-((4-Chlorophenyl)amino)thiazole-4-carboxylic acid. **Scheme 1**, general procedure C, using 1-

(4-chlorophenyl)thiourea. Brown solid, 76% yield (289.1 mg). Decomposes at 242.7 °C. ¹H NMR (600 MHz, (CD₃)₂SO) δ ppm 12.73 (br. s, 1 H), 10.50 (s, 1 H), 7.74 (s, 1 H), 7.71 (m, 2 H), 7.37 (m, 2 H). ¹³C NMR (151 MHz, (CD₃)₂SO) δ ppm 162.5, 162.1, 143.4, 139.7, 128.8, 124.8, 118.6, 118.4. HRMS (ESI-TOF) calcd for C₁₀H₈ClN₂O₂S: 254.9990, found 254.9991 [M+H]⁺.

Scheme 1, general procedure E and F, using 4-chloroaniline. White solid, 96% yield (437 mg).

2-((4-Chloro-3-fluorophenyl)amino)thiazole-4-carboxylic acid. **Scheme 1**, general procedure C, using 1-(4-chloro-3-fluorophenyl)thiourea. Brown solid, 88% yield (405.9 mg). Decomposes at 233.9 °C. ¹H NMR (600 MHz, (CD₃)₂SO) δ ppm 12.73 (br. s, 1 H), 10.98 (br. s, 1 H), 8.02 (dd, *J* = 12.2, 2.2 Hz, 1 H), 7.78 (s, 1 H), 7.49 (t, *J* = 8.7 Hz, 1 H), 7.37 (d, *J* = 8.7 Hz, 1 H). ¹³C NMR (151 MHz, (CD₃)₂SO) δ ppm 162.1, 162.0, 157.2 (d, *J* = 243.2 Hz), 143.4, 141.3 (d, *J* = 11.0 Hz), 130.5, 119.2, 113.9 (d, *J* = 3.3 Hz), 110.4 (d, *J* = 17.6 Hz), 104.9 (d, *J* = 26.4 Hz). HRMS (ESI-TOF) calcd for C₁₀H₇ClFN₂O₂S: 272.9895, found 272.9897 [M+H]⁺.

2-((4-Chloro-3,5-difluorophenyl)amino)thiazole-4-carboxylic acid. **Scheme 1**, general procedure C, using 1-(4-chloro-3,5-difluorophenyl)thiourea. Light brown solid, 96% yield (4.7515 g). Decomposes at 290.6 °C. ¹H NMR (600 MHz, (CD₃)₂SO) δ ppm 12.85 (br. s, 1 H), 11.50 (s, 1 H), 7.82 (s, 1 H), 7.71 (d, *J* = 10.0 Hz, 2 H). ¹³C NMR (151 MHz, (CD₃)₂SO) δ ppm 161.9 (d, *J* = 8.8 Hz), 158.9 (d, *J* = 5.5 Hz), 157.3 (d, *J* = 5.5 Hz), 143.2, 141.1 (t, *J* = 13.8 Hz), 119.7, 100.7 (d, *J* = 28.6 Hz), 98.9 (t, *J* = 22.0 Hz). HRMS (ESI-TOF) calcd for C₁₀H₆ClF₂N₂O₂S: 290.9801, found 290.9802 [M+H]⁺.

2-Chloro-N-(3-morpholinopropyl)thiazole-4-carboxamide. **Scheme 1**, general procedure H, using 2-chlorothiazole-4-carboxylic acid and N-(3-aminopropyl)morpholine. Pale orange solid, 71% yield (697.0 mg). *R*_f = 0.43 (5% MeOH in DCM). m.p. 75.8–78.6 °C. ¹H NMR (600 MHz, CDCl₃) δ ppm 8.72 (br. s, 1 H), 7.98 (s, 1 H), 3.87 (t, *J* = 4.6 Hz, 4 H), 3.55 (q, *J* = 5.9 Hz, 2 H), 2.54 (m, 6 H), 1.79 (quint, *J* = 6.1 Hz, 2 H). ¹³C NMR (151 MHz, CDCl₃) δ ppm 159.9, 151.5, 148.8, 124.5, 66.6, 58.4, 53.8, 39.8, 24.4. HRMS (ESI-TOF) calcd for C₁₁H₁₇ClN₃O₂S: 290.0724, found 290.0726 [M+H]⁺.

2-Chloro-N-(3-isopropoxypropyl)thiazole-4-carboxamide. **Scheme 1**, general procedure H, using 2-chlorothiazole-4-carboxylic acid and 3-isopropoxypropylamine. Yellow oil, 74% yield (545.7 mg). *R*_f = 0.57 (5% MeOH in DCM). ¹H NMR (500 MHz, CDCl₃) δ ppm 7.97 (s, 1 H), 7.92 (br. s, 1 H), 3.58 (m, 5 H), 1.86 (quint, *J* = 5.9 Hz, 2 H), 1.22 (d, *J* = 6.2 Hz, 6 H). ¹³C NMR (151 MHz, CDCl₃) δ ppm 159.7, 151.4, 148.8, 124.4, 71.9, 67.2, 38.6, 29.1, 22.0. HRMS (ESI-TOF) calcd for C₁₀H₁₆ClN₂O₂S: 263.0615, found 263.0617 [M+H]⁺.

2-Chloro-N-(3-ethoxypropyl)thiazole-4-carboxamide. **Scheme 1**, general procedure H, using 2-chlorothiazole-4-carboxylic acid and 3-ethoxypropylamine. Off-white solid, 78% yield (547.3 mg). *R*_f = 0.36 (5% MeOH in DCM). m.p. 76.7–79.4 °C. ¹H NMR (500 MHz, CDCl₃) δ ppm 7.97 (s, 1 H), 7.82 (br. s, 1 H), 3.54 (m, 6 H), 1.87 (quin, *J* = 5.9 Hz, 2 H), 1.28 (t, *J* = 7.0 Hz, 3 H). ¹³C NMR (151 MHz, CDCl₃) δ ppm 159.7, 151.4, 148.7, 124.5, 69.6, 66.5, 38.3, 29.0, 15.2. HRMS (ESI-TOF) calcd for C₉H₁₄ClN₂O₂S: 249.0459, found 249.0457 [M+H]⁺.

N-(3-Morpholinopropyl)-2-(3,4-dichlorophenyl-amino)thiazole-4-carboxamide (1). **Scheme 1**, general procedure G, using 2-((3,4-dichlorophenyl)amino)thiazole-4-carboxylic acid and 3-morpholinopropylamine. Column chromatography (MeOH/CH₂Cl₂, 1:39 to 1:19). White solid, 72% yield (299 mg). *R*_f = 0.33 (MeOH/CH₂Cl₂ = 1:19). m.p. 108–109 °C. IR ν_{max} (neat) 2920, 2850, 1620, 1550, 1475 cm⁻¹. ¹H NMR (600 MHz, CDCl₃) δ ppm 9.34 (s, 1 H), 7.76 (d, *J* = 2.4 Hz, 1 H), 7.72 (t, *J* = 6.6 Hz, 1 H), 7.40 (s, 1 H), 7.33 (dd, *J* = 9.0, 2.4 Hz, 1 H), 7.28 (d, *J* = 9.0 Hz, 1 H), 3.61 (t, *J* = 4.2 Hz, 4 H), 3.49 (q, *J* = 6.6 Hz, 2 H), 2.41–2.37 (m, 6 H), 1.74 (quint, *J* = 6.6 Hz, 2 H). ¹³C NMR (150 MHz, CDCl₃) δ ppm 163.2, 161.6, 145.6, 139.9, 132.5, 130.4, 124.9, 119.2, 117.0, 113.6, 66.6 (× 2), 56.7, 53.5 (× 2), 38.3, 25.8. HRMS (ESI) calcd for C₁₇H₂₁Cl₂N₄O₂S: 415.0757, found: 415.0837 [M + H]⁺.

2-((3,4-Dichlorophenyl)amino)-N-(3-isopropoxy-propyl)thiazole-4-carboxamide (11). **Scheme 1**, general procedure D, using 2-((3,4-dichlorophenyl)amino)thiazole-4-carboxylic acid and 3-isopropoxypropylamine. Light orange solid, 23% yield (66.9 mg). *R*_f = 0.51 (5% MeOH in DCM).

m.p. 119.7–124.1 °C. ¹H NMR (600 MHz, CDCl₃) δ ppm 8.28 (br.s., 1 H), 7.70 (d, *J* = 2.6 Hz, 1 H), 7.56 (t, *J* = 5.8 Hz, 1 H), 7.47 (s, 1 H), 7.39 (d, *J* = 8.7 Hz, 1 H), 7.34 (dd, *J* = 9.0, 2.6 Hz, 1 H), 3.58 (m, 5 H), 1.88 (quint, *J* = 6.2 Hz, 2 H), 1.15 (d, *J* = 6.2 Hz, 6 H). ¹³C NMR (151 MHz, CDCl₃) δ ppm 163.1, 161.4, 146.1, 139.7, 132.9, 130.8, 125.7, 119.6, 117.3, 113.5, 71.8, 66.3, 37.8, 29.7, 22.1. HRMS (ESI-TOF) calcd for C₁₆H₂₀Cl₂N₃O₂S: 388.0648, found 388.0651 [M+H]⁺.

2-((3,4-Dichlorophenyl)amino)-*N*-(3-ethoxypropyl)thiazole-4-carboxamide (12). Scheme 1, general procedure D, using 2-((3,4-dichlorophenyl)amino)thiazole-4-carboxylic acid and 3-ethoxypropylamine. Off-white solid, 37% yield (109.9 mg). *R*_f = 0.51 (5% MeOH in DCM). m.p. 139.1–143.7 °C. ¹H NMR (600 MHz, CDCl₃) δ ppm 8.42 (br. s, 1 H), 7.72 (d, *J* = 2.3 Hz, 1 H), 7.59 (t, *J* = 5.7 Hz, 1 H), 7.47 (s, 1 H), 7.38 (m, 2 H), 3.58 (m, 4 H), 3.51 (q, *J* = 7.0 Hz, 2 H), 1.90 (quint, *J* = 6.2 Hz, 2 H), 1.19 (t, *J* = 6.9 Hz, 3 H). ¹³C NMR (151 MHz, CDCl₃) δ ppm 163.1, 161.4, 146.1, 139.7, 132.9, 130.7, 125.6, 119.5, 117.2, 113.5, 68.9, 66.4, 37.8, 29.4, 15.1. HRMS (ESI-TOF) calcd for C₁₅H₁₈Cl₂N₃O₂S: 374.0491, found 374.0495 [M+H]⁺.

2-(3,4,5-Trichlorophenylamino)-*N*-(3-morpholino-propyl)thiazole-4-carboxamide (13). Scheme 1, general procedure G, using 2-((3,4,5-trichlorophenyl)amino)thiazole-4-carboxylic acid and *N*-(3-aminopropyl)morpholine. Silica gel column chromatography (CH₂Cl₂/2.5–5% MeOH). White solid, 79% yield (708 mg). *R*_f = 0.34 (MeOH/CH₂Cl₂, 1:19). m.p. 164–165 °C. ¹H NMR (600 MHz, CDCl₃) δ ppm 9.07 (s, 1 H), 7.75 (t, *J* = 6.0 Hz, 1 H), 7.65 (s, 2 H), 7.46 (s, 1 H), 3.66 (m, 4 H), 3.54 (q, *J* = 6.0 Hz, 2 H), 2.45 (m, 6 H), 1.79 (quint, *J* = 6.0 Hz, 2 H). ¹³C NMR (150 MHz, CDCl₃) δ ppm 162.7, 161.5, 145.9, 139.6, 134.2, 124.0, 117.6, 114.2, 66.8, 57.0, 53.7, 38.5, 25.8. HRMS (ESI-TOF) calcd for C₁₇H₂₀Cl₃N₄O₂S: 449.0367, found 449.0376 [M+H]⁺.

***N*-(3-Isopropoxypropyl)-2-((3,4,5-trichlorophenyl)amino)thiazole-4-carboxamide (14).** Scheme 1, general procedure D, using 2-((3,4,5-trichlorophenyl)amino)thiazole-4-carboxylic acid and 3-isopropoxypropylamine. Light red solid, 53% yield (168.5 mg). *R*_f = 0.51 (5% MeOH in DCM). m.p. 173.9–178.5 °C. ¹H NMR (600 MHz, CDCl₃) δ

ppm 8.33 (br. s, 1 H), 7.64 (s, 2 H), 7.56 (m, 1 H), 7.51 (s, 1 H), 3.58 (m, 5 H), 1.90 (quint, *J* = 6.2 Hz, 2 H), 1.15 (d, *J* = 5.9 Hz, 6 H). ¹³C NMR (151 MHz, CDCl₃) δ ppm 162.5, 161.3, 146.2, 139.4, 134.4, 124.4, 117.8, 114.0, 71.8, 66.3, 37.9, 29.6, 22.1. HRMS (ESI-TOF) calcd C₁₆H₁₉Cl₃N₃O₂S: 422.0258, found 422.0265 [M+H]⁺.

***N*-(3-Ethoxypropyl)-2-((3,4,5-trichlorophenyl)amino)thiazole-4-carboxamide (15).** Scheme 1, general procedure D, using 2-((3,4,5-trichlorophenyl)amino)thiazole-4-carboxylic acid and 3-ethoxypropylamine. Light brown solid, 25% yield (52.6 mg). *R*_f = 0.46 (5% MeOH in DCM). m.p. 171.6–177.0 °C. ¹H NMR (600 MHz, (CD₃)₂CO) δ ppm 9.76 (br. s, 1 H), 7.92 (s, 2 H), 7.79 (m, 1 H), 7.55 (s, 1 H), 3.52 (t, *J* = 6.0 Hz, 2 H), 3.46 (m, 4 H), 1.84 (quint, *J* = 6.4 Hz, 2 H), 1.11 (t, *J* = 6.9 Hz, 3 H). ¹³C NMR (151 MHz, (CD₃)₂CO) δ ppm 153.5, 151.5, 138.1, 131.7, 124.7, 113.3, 108.5, 104.8, 59.4, 56.9, 28.0, 20.8, 5.7. HRMS (ESI-TOF) calcd for C₁₅H₁₇Cl₃N₃O₂S: 408.0102, found 408.0101 [M+H]⁺.

2-(4-Chlorophenylamino)-*N*-(3-morpholinopropyl)thiazole-4-carboxamide (16). Scheme 1, general procedure G, using 2-((4-chlorophenyl)amino)thiazole-4-carboxylic acid and *N*-(3-aminopropyl)morpholine. Silica gel column chromatography (CH₂Cl₂/2.5–5% MeOH). White solid, 72% yield (299 mg). *R*_f = 0.31 (MeOH/CH₂Cl₂, 1:19). m.p. 130–131 °C. ¹H NMR (600 MHz, CDCl₃) δ ppm 8.94 (s, 1 H), 7.73 (t, *J* = 6.6 Hz, 1 H), 7.41 (d, *J* = 8.4 Hz, 2 H), 7.21 (d, *J* = 8.4 Hz, 2 H), 3.63 (t, *J* = 4.2 Hz, 4 H), 3.46 (q, *J* = 6.6 Hz, 2 H), 2.38 (m, 6 H), 1.72 (quint, *J* = 6.6 Hz, 2 H). ¹³C NMR (150 MHz, CDCl₃) δ ppm 163.9, 161.6, 145.7, 138.9, 129.0, 127.3, 119.3, 113.0, 66.6, 56.7, 53.5, 38.2, 25.8. HRMS (ESI-TOF) calcd for C₁₇H₂₂ClN₄O₂S: 381.1147, found 381.1143 [M+H]⁺.

2-((4-Chlorophenyl)amino)-*N*-(3-isopropoxypropyl)thiazole-4-carboxamide (17). Scheme 1, general procedure D, using 2-((4-chlorophenyl)amino)thiazole-4-carboxylic acid and 3-isopropoxypropylamine. Off-white solid, 28% yield (110.3 mg). *R*_f = 0.54 (5% MeOH in DCM). m.p. 148.7–151.8 °C. ¹H NMR (600 MHz, CDCl₃) δ ppm 7.80 (s, 1 H), 7.54 (t, *J* = 5.5 Hz, 1 H), 7.44 (s, 1 H), 7.39 (m, 2 H), 7.31 (m, 2 H), 3.57 (m, 5 H), 1.87 (quint, *J* = 6.2 Hz, 2 H), 1.17 (d, *J* = 6.2 Hz, 6 H). ¹³C

NMR (151 MHz, CDCl_3) δ ppm 163.8, 161.4, 146.2, 138.7, 129.4, 128.1, 119.6, 112.9, 71.7, 66.4, 37.7, 29.7, 22.1. HRMS (ESI-TOF) calcd for $\text{C}_{16}\text{H}_{21}\text{ClN}_3\text{O}_2\text{S}$ $[\text{M}+\text{H}]^+$: 354.1037, found 354.1040.

2-((4-Chlorophenyl)amino)-*N*-(3-ethoxypropyl)thiazole-4-carboxamide (18). Scheme 1, general procedure D, using 2-((4-chlorophenyl)amino)thiazole-4-carboxylic acid and 3-ethoxypropylamine. Orange solid, 49% yield (126.2 mg). R_f = 0.21 (5% MeOH in DCM). m.p. 138.2-142.5 °C. ^1H NMR (600 MHz, $(\text{CD}_3)_2\text{CO}$) δ ppm 9.62 (br. s, 1 H), 7.84 (br. s, 1 H), 7.76 (m, 2 H), 7.47 (s, 1 H), 7.30 (m, 2 H), 3.50 (t, J = 6.0 Hz, 2 H), 3.46 (m, 4 H), 1.83 (quint, J = 6.5 Hz, 2 H), 1.13 (t, J = 6.9 Hz, 3 H). ^{13}C NMR (151 MHz, $(\text{CD}_3)_2\text{SO}$) δ ppm 162.7, 160.5, 146.1, 139.7, 128.7, 124.7, 118.7, 113.2, 67.9, 65.4, 36.6, 29.6, 15.1. HRMS (ESI-TOF) calcd for $\text{C}_{15}\text{H}_{19}\text{ClN}_3\text{O}_2\text{S}$: 340.0881, found 340.0881 $[\text{M}+\text{H}]^+$.

2-((4-Chloro-3-methylphenyl)amino)-*N*-(3-morpholinopropyl)thiazole-4-carboxamide (19). Scheme 1, general procedure I, using 2-chloro-*N*-(3-morpholinopropyl)thiazole-4-carboxamide and 4-chloro-3-methylaniline. Red solid, 45% yield (99.2 mg). R_f = 0.38 (5% MeOH in DCM). m.p. 67.8-79.4 °C. ^1H NMR (600 MHz, $(\text{CD}_3)_2\text{CO}$) δ ppm 9.59 (br. s, 1 H), 7.92 (t, J = 5.3 Hz, 1 H), 7.65 (dd, J = 8.7, 2.6 Hz, 1 H), 7.56 (d, J = 2.3 Hz, 1 H), 7.49 (s, 1 H), 7.27 (d, J = 8.5 Hz, 1 H), 3.58 (m, 4 H), 3.45 (q, J = 6.7 Hz, 2 H), 2.39 (m, 6 H), 2.33 (s, 3 H), 1.77 (quin, J = 6.9 Hz, 2 H). ^{13}C NMR (151 MHz, $(\text{CD}_3)_2\text{CO}$) δ ppm 164.5, 161.9, 147.7, 140.8, 137.2, 130.2, 127.4, 120.9, 117.7, 113.6, 67.4, 57.5, 54.7, 38.6, 27.2, 20.4. HRMS (ESI-TOF) calcd for $\text{C}_{18}\text{H}_{24}\text{ClN}_4\text{O}_2\text{S}$: 395.1303, found 395.1305 $[\text{M}+\text{H}]^+$.

2-((4-Chloro-3-methylphenyl)amino)-*N*-(3-isopropoxypropyl)thiazole-4-carboxamide (20). Scheme 1, general procedure I, using 2-chloro-*N*-(3-isopropoxypropyl)thiazole-4-carboxamide and 4-chloro-3-methylaniline. Orange solid, 33% yield (95.4 mg). R_f = 0.49 (5% MeOH in DCM). m.p. 127.0-130.9 °C. ^1H NMR (600 MHz, $(\text{CD}_3)_2\text{CO}$) δ ppm 9.48 (br. s, 1 H), 7.79 (t, J = 5.1 Hz, 1 H), 7.64 (dd, J = 8.7, 2.6 Hz, 1 H), 7.59 (d, J = 2.3 Hz, 1 H), 7.46 (s, 1 H), 7.27 (d, J = 8.7 Hz, 1 H), 3.55 (spt, J = 6.2 Hz, 1 H), 3.51 (t, J = 6.0 Hz, 2 H), 3.46 (q, J = 6.7 Hz, 2 H), 2.34 (s, 3 H), 1.82 (quint, J = 6.4 Hz, 2 H), 1.09 (d, J =

6.2 Hz, 6 H). ^{13}C NMR (151 MHz, $(\text{CD}_3)_2\text{CO}$) δ ppm 154.5, 151.7, 138.0, 130.9, 127.3, 120.3, 117.4, 111.0, 107.7, 103.4, 62.2, 56.9, 28.0, 21.1, 12.6, 10.5. HRMS (ESI-TOF) calcd for $\text{C}_{17}\text{H}_{23}\text{ClN}_3\text{O}_2\text{S}$: 368.1194, found 368.1194 $[\text{M}+\text{H}]^+$.

2-((4-Chloro-3-methylphenyl)amino)-*N*-(3-ethoxypropyl)thiazole-4-carboxamide(21). Scheme 1, general procedure I, using 2-chloro-*N*-(3-ethoxypropyl)thiazole-4-carboxamide and 4-chloro-3-methylaniline. Orange solid, 33% yield (91.8 mg). R_f = 0.53 (5% MeOH in DCM). m.p. 108.8-112.6 °C. ^1H NMR (500 MHz, $(\text{CD}_3)_2\text{CO}$) δ ppm 9.55 (br. s, 1 H), 7.85 (m, 1 H), 7.65 (dd, J = 8.6, 2.4 Hz, 1 H), 7.59 (s, 1 H), 7.47 (s, 1 H), 7.27 (d, J = 8.7 Hz, 1 H), 3.51 (t, J = 6.2 Hz, 2 H), 3.46 (m, 4 H), 2.34 (s, 3 H), 1.84 (quint, J = 6.4 Hz, 2 H), 1.12 (t, J = 6.9 Hz, 3 H). ^{13}C NMR (151 MHz, $(\text{CD}_3)_2\text{CO}$) δ ppm 164.4, 161.8, 147.8, 140.8, 137.2, 130.2, 127.3, 120.8, 117.6, 113.4, 69.4, 66.7, 38.0, 30.7, 20.4, 15.6. HRMS (ESI-TOF) calcd for $\text{C}_{16}\text{H}_{21}\text{ClN}_3\text{O}_2\text{S}$: 354.1037, found 354.1038 $[\text{M}+\text{H}]^+$.

2-((4-Chloro-3,5-dimethylphenyl)amino)-*N*-(3-morpholinopropyl)thiazole-4-carboxamide (22). Scheme 1, general procedure I, using 2-chloro-*N*-(3-morpholinopropyl)thiazole-4-carboxamide and 4-chloro-3,5-dimethylaniline. Pale yellow solid, 34% yield (79.5 mg). R_f = 0.19 (5% MeOH in DCM). m.p. 137.5-142.3 °C. ^1H NMR (600 MHz, CDCl_3) δ ppm 7.87 (m, 1 H), 7.53 (br. s, 1 H), 7.43 (s, 1 H), 7.10 (s, 2 H), 3.75 (m, 4 H), 3.52 (q, J = 6.3 Hz, 2 H), 2.47 (m, 6 H), 2.38 (s, 6 H), 1.78 (quint, J = 6.6, 2 H). ^{13}C NMR (151 MHz, CDCl_3) δ ppm 164.6, 161.4, 146.1, 137.7, 137.4, 129.3, 118.8, 112.6, 66.8, 57.3, 53.7, 38.6, 26.8, 21.0. HRMS (ESI-TOF) calcd for $\text{C}_{19}\text{H}_{26}\text{ClN}_4\text{O}_2\text{S}$: 409.1459, found 409.1458 $[\text{M}+\text{H}]^+$.

2-((4-Chloro-3,5-dimethylphenyl)amino)-*N*-(3-isopropoxypropyl)thiazole-4-carboxamide (23). Scheme 1, general procedure I, using 2-chloro-*N*-(3-isopropoxypropyl)thiazole-4-carboxamide and 4-chloro-3,5-dimethylaniline. Pale yellow solid, 51% yield (93.0 mg). R_f = 0.28 (5% MeOH in DCM). m.p. 147.7-151.0 °C. ^1H NMR (500 MHz, $(\text{CD}_3)_2\text{CO}$) δ ppm 9.35 (br. s, 1 H), 7.74 (m, 1 H), 7.49 (s, 2 H), 7.44 (s, 1 H), 3.55 (m, 3 H), 3.46 (q, J = 6.7 Hz, 2 H), 2.35 (s, 6 H), 1.83 (quint, J = 6.4 Hz, 2 H), 1.09 (d, J = 6.2 Hz, 6 H). ^{13}C NMR (151 MHz, $(\text{CD}_3)_2\text{CO}$) δ ppm 164.5, 161.7, 147.9, 140.1, 137.5,

127.9, 118.7, 113.1, 72.1, 66.9, 38.0, 31.0, 22.5, 21.1. HRMS (ESI-TOF) calcd for $C_{18}H_{25}ClN_3O_2S$: 382.1350, found 382.1350 $[M+H]^+$.

2-((4-Chloro-3,5-dimethylphenyl)amino)-*N*-(3-ethoxypropyl)thiazole-4-carboxamide (24). Scheme 1, general procedure I, using 2-chloro-*N*-(3-ethoxypropyl)thiazole-4-carboxamide and 4-chloro-3,5-dimethylaniline. Pale yellow solid, 29% yield (53.8 mg). R_f = 0.49 (5% MeOH in DCM). m.p. 137.1-142.0 °C. 1H NMR (500 MHz, $(CD_3)_2CO$) δ ppm 9.35 (br. s, 1 H), 7.76 (m, 1 H), 7.50 (s, 2 H), 7.44 (s, 1 H), 3.53 (t, J = 6.2 Hz, 2 H), 3.46 (m, 4 H), 2.35 (s, 6 H), 1.85 (quint, J = 6.4 Hz, 2 H), 1.11 (t, J = 6.9 Hz, 3 H). ^{13}C NMR (151 MHz, $(CD_3)_2CO$) δ ppm 164.5, 161.6, 147.9, 140.1, 137.5, 127.9, 118.7, 113.1, 69.4, 66.7, 37.9, 30.6, 21.1, 15.6. HRMS (ESI-TOF) calcd for $C_{17}H_{23}ClN_3O_2S$: 368.1194, found 368.1192 $[M+H]^+$.

2-((4-Chloro-3-fluorophenyl)amino)-*N*-(3-morpholinopropyl)thiazole-4-carboxamide (25). Scheme 1, general procedure I, using 2-chloro-*N*-(3-morpholinopropyl)thiazole-4-carboxamide and 4-chloro-3-fluoroaniline. Dark orange solid, 48% yield (81.3 mg). R_f = 0.35 (5% MeOH in DCM). m.p. 58.0-69.3 °C. 1H NMR (600 MHz, $(CD_3)_2CO$) δ ppm 9.80 (br. s, 1 H), 7.97 (br. s, 1 H), 7.89 (dd, J = 11.7, 2.2 Hz, 1 H), 7.54 (s, 1 H), 7.40 (m, 2 H), 3.59 (m, 4 H), 3.45 (q, J = 6.7 Hz, 2 H), 2.40 (m, 6 H), 1.78 (quint, J = 6.7 Hz, 2 H). ^{13}C NMR (151 MHz, $(CD_3)_2CO$) δ ppm 163.9, 161.6, 158.1 (d, J = 244.3 Hz), 148.0, 142.4 (d, J = 12.1 Hz), 131.5, 115.2 (d, J = 3.3 Hz), 114.3, 112.8 (d, J = 17.6 Hz), 106.6 (d, J = 26.4 Hz), 67.4, 57.5, 54.7, 38.5, 27.3. HRMS (ESI-TOF) calcd for $C_{17}H_{21}ClFN_4O_2S$: 399.1052, found 399.1049 $[M+H]^+$.

2-((4-Chloro-3-fluorophenyl)amino)-*N*-(3-isopropoxypropyl)thiazole-4-carboxamide(26). Scheme 1, general procedure D, using 2-((4-chloro-3-fluorophenyl)amino)thiazole-4-carboxylic acid and 3-isopropoxypropylamine. Light brown solid, 59% yield (251.0 mg). R_f = 0.43 (5% MeOH in DCM). m.p. 143.9-147.1 °C. 1H NMR (600 MHz, $CDCl_3$) δ ppm 8.65 (m, 1 H), 7.57 (m, 2 H), 7.47 (m, 1 H), 7.32 (m, 1 H), 7.16 (m, 1 H), 3.57 (m, 5 H), 1.88 (quint, J = 6.2 Hz, 2 H), 1.15 (m, 6 H). ^{13}C NMR (151 MHz, $CDCl_3$) δ ppm 163.1 (m), 161.5 (m), 159.1, 157.4, 146.0 (d, J = 4.4 Hz), 140.3 (m), 130.7, 114.1, 113.6,

106.3 (d, J = 26.4 Hz), 71.8, 66.2, 37.8, 29.7, 22.0. HRMS (ESI-TOF) calcd for $C_{16}H_{20}ClFN_3O_2S$: 372.0943, found 372.0948 $[M+H]^+$.

2-((4-Chloro-3-fluorophenyl)amino)-*N*-(3-ethoxypropyl)thiazole-4-carboxamide(27). Scheme 1, general procedure D, using 2-((4-chloro-3-fluorophenyl)amino)thiazole-4-carboxylic acid and 3-ethoxypropylamine. Orange solid, 57% yield (166.1 mg). R_f = 0.25 (5% MeOH in DCM). m.p. 150.6-154.8 °C. 1H NMR (600 MHz, $(CD_3)_2SO$) δ ppm 10.63 (br. s, 1 H), 8.19 (t, J = 5.9 Hz, 1 H), 7.93 (dd, J = 12.1, 2.8 Hz, 1 H), 7.55 (s, 1 H), 7.45 (t, J = 8.5 Hz, 1 H), 7.38 (dd, J = 8.9, 2.2 Hz, 1 H), 3.42 (m, 4 H), 3.32 (q, J = 6.4 Hz, 2 H), 1.76 (quint, J = 6.6 Hz, 2 H), 1.09 (t, J = 7.1 Hz, 3 H). ^{13}C NMR (151 MHz, $(CD_3)_2SO$) δ ppm 162.3, 160.5, 157.3 (d, J = 244.3 Hz), 146.3, 141.1 (d, J = 9.9 Hz), 130.5, 114.1 (d, J = 3.3 Hz), 113.8, 110.6 (d, J = 17.6 Hz), 105.2 (d, J = 26.4 Hz), 67.9, 65.4, 36.6, 29.5, 15.1. HRMS (ESI-TOF) calcd for $C_{15}H_{18}ClFN_3O_2S$: 358.0787, found 358.0788 $[M+H]^+$.

2-((4-Chloro-3,5-difluorophenyl)amino)-*N*-(3-morpholinopropyl)thiazole-4-carboxamide (28). Scheme 1, general procedure D, using 2-((4-chloro-3,5-difluorophenyl)amino)thiazole-4-carboxylic acid and *N*-(3-aminopropyl)morpholine. Orange solid, 61% yield (145.6 mg). R_f = 0.43 (5% MeOH in DCM). m.p. 139.9-146.3 °C. 1H NMR (600 MHz, $(CD_3)_2CO$) δ ppm 8.01 (m, 1 H), 7.57 (m, 3 H), 3.58 (m, 4 H), 3.45 (q, J = 6.9 Hz, 2 H), 2.40 (m, 6 H), 1.77 (quint, J = 6.9 Hz, 2 H). ^{13}C NMR (151 MHz, $(CD_3)_2CO$) δ ppm 163.5, 161.5 (m), 160.6 (d, J = 5.5 Hz), 159.0 (d, J = 5.5 Hz), 148.1, 142.1 (t, J = 13.2 Hz), 114.8, 102.2 (m), 102.0 (m), 101.3 (t, J = 22.0 Hz), 67.5, 57.5, 54.7, 38.5, 27.3. HRMS (ESI-TOF) calcd for $C_{17}H_{20}ClF_2N_4O_2S$: 417.0958, found 417.0958 $[M+H]^+$.

2-((4-Chloro-3,5-difluorophenyl)amino)-*N*-(3-isopropoxypropyl)thiazole-4-carboxamide (29). Scheme 1, general procedure D, using 2-((4-chloro-3,5-difluorophenyl)amino)thiazole-4-carboxylic acid and 3-isopropoxypropylamine. Light brown solid, 72% yield (205.3 mg). R_f = 0.40 (5% MeOH in DCM). m.p. 149.9-154.8 °C. 1H NMR (600 MHz, $(CD_3)_2CO$) δ ppm 9.96 (br. s, 1 H), 7.95 (m, 1 H), 7.58 (m, 3 H), 3.55 (spt, J = 6.1 Hz, 1 H), 3.50 (t, J = 6.1 Hz, 2 H), 3.46 (q, J = 6.9 Hz, 2 H), 1.81 (quint, J

= 6.7 Hz, 2 H), 1.09 (d, J = 6.2 Hz, 6 H). ^{13}C NMR (151 MHz, $(\text{CD}_3)_2\text{SO}$) δ ppm 162.0, 160.4, 159.0 (d, J = 5.5 Hz), 157.4 (d, J = 5.5 Hz), 146.4, 140.8 (t, J = 13.2 Hz), 114.3, 101.1 (d, J = 28.6 Hz), 99.2 (t, J = 22.0 Hz), 70.7, 65.4, 36.6, 29.8, 22.0. HRMS (ESI-TOF) calcd for $\text{C}_{16}\text{H}_{19}\text{ClF}_2\text{N}_3\text{O}_2\text{S}$: 390.0849, found 390.0850 $[\text{M}+\text{H}]^+$. For synthesis of the salt compound used in *in vivo* studies, anhydrous 1,4-dioxane (0.13 M) was added to 2-((4-chloro-3,5-difluorophenyl)amino)-*N*-(3-isopropoxypropyl)thiazole-4-carboxamide (compound **29**, 1.0 equiv) and heated or sonicated until completely dissolved. While stirring, concentrated sulfuric acid (2.0 equiv) was added dropwise and the mixture stirred at room temperature for 2 hours. The final product (dark orange solid, 99% yield) was obtained by concentrating the mixture under reduced pressure until completely dry.

2-((4-Chloro-3,5-difluorophenyl)amino)-*N*-(3-ethoxypropyl)thiazole-4-carboxamide (30). Scheme 1, general procedure D, using 2-((4-chloro-3,5-difluorophenyl)amino)thiazole-4-carboxylic acid and 3-ethoxypropylamine. Off-white solid, 43% yield (128.2 mg). R_f = 0.37 (5% MeOH in DCM). m.p. 180.2–183.9 °C. ^1H NMR (600 MHz, $(\text{CD}_3)_2\text{SO}$) δ ppm 10.8 (s, 1 H), 8.27 (t, J = 5.9 Hz, 1 H), 7.59 (m, 3 H), 3.41 (m, 4 H), 3.33 (q, J = 6.7 Hz, 2 H), 1.76 (quint, J = 6.6 Hz, 2 H), 1.09 (t, J = 7.1 Hz, 3 H). ^{13}C NMR (151 MHz, $(\text{CD}_3)_2\text{SO}$) δ ppm 162.0, 160.4, 159.0 (d, J = 5.5 Hz), 157.3 (d, J = 5.5 Hz), 146.4, 140.7 (t, J = 13.2 Hz), 114.4, 101.1 (m), 101.0 (m), 99.2 (t, J = 22.0 Hz), 67.9, 65.4, 36.6, 29.5, 15.1. HRMS (ESI-TOF) calcd for $\text{C}_{15}\text{H}_{17}\text{ClF}_2\text{N}_3\text{O}_2\text{S}$: 376.0693, found 376.0692 $[\text{M}+\text{H}]^+$. For synthesis of the salt compounds used in *in vivo* studies, anhydrous ethyl acetate (0.05 M) was added to 2-((4-chloro-3,5-difluorophenyl)amino)-*N*-(3-ethoxypropyl)thiazole-4-carboxamide (compound **30**, 1.0 equiv) and heated or sonicated until completely dissolved. While stirring, methane sulfonic acid (2.0 equiv) was added dropwise and the mixture stirred at room temperature for 2 hours. The final product (orange solid, 98% yield) was obtained by concentrating the mixture under reduced pressure until completely dry.

Viruses, cells, and biological reagents. Recombinant virus Influenza A/WSN/1933 (H1N1) (NA wt), Influenza A/WSN/1933 (H1N1) (NA H274Y), Influenza RG14 (H5N1) harboring the hemagglutinin and neuraminidase from A/Viet

Nam/1194/2004 (H5N1) (NA wt), Influenza RG14 (H5N1) (NA H274Y) were produced by using plasmids provided by Dr. King-Song Jeng (Institute of Molecular Biology, Academia Sinica). The attenuated reassortant H1N1 influenza viruses A/California/7/2009 was from the National Institute for Biological Standards and Control. Influenza A/Mississippi (A/New Caledonia/20/99-like) (wt), Influenza A/Mississippi (A/New Caledonia/20/99-like) (H274Y), A/Perth (H1N1pdm09) (wt), and A/Perth (H1N1pdm09) (H275Y) were obtained from World Health Organization (WHO). Influenza B/Florida were kindly provided from Dr. Che Ma (Genomics Research Center, Academia Sinica). All viruses were cultured either by using Madin–Darby canine kidney (MDCK) cells or in the allantoic cavities of 10-day-old embryonated chicken eggs for 72 hours. MDCK cells were obtained from American Type Culture Collection (Manassas, VA), and were grown in DMEM (Dulbecco's Modified Eagle Medium, GibcoBRL) containing 10% fetal bovine serum (GibcoBRL) and penicillin–streptomycin (GibcoBRL) at 37 °C under 5% CO_2 . All cell culture reagents were obtained from Invitrogen Inc. (Carlsbad, CA, USA).

Determination of EC_{50} and CC_{50} values of small molecules. The anti-influenza activities of compounds were measured by the EC_{50} values, which were the concentrations of tested molecules for 50% protection of the influenza virus infection-mediated cytopathic effects (CPE). Fifty microliters of diluted influenza virus at 100 TCID_{50} was mixed with equal volumes of compounds at varied concentrations. The mixtures were used to infect 100 μL of MDCK cells at 1×10^5 cells/mL in 96 wells. After 48 hours of incubation at 37 °C under 5% CO_2 , the cytopathic effects were determined with CellTiter 96 AQueous Non-Radioactive Cell Proliferation Assay reagent (Promega). The EC_{50} values were determined by fitting the curve of percent CPE versus the concentrations of compounds using Graph Pad Prism 4. The CC_{50} values (50% cytotoxic concentrations) of compounds to MDCK cells were determined by the procedures analogous to the EC_{50} determination but without virus infection.

Animal experiments for virus challenges. Female BALB/c mice (18–20 g) were obtained from Charles River Laboratories or National Laboratory Animal Center (Taiwan). All animal experiments were evaluated and approved by the Institutional

Animal Care and Use Committee of Academia Sinica, Taiwan. The mice were quarantined for 48–72 hours before use. The mice were anesthetized by intraperitoneal injection of zoletil (or ketamine/xylazine) and inoculated intranasally with 25 μ L of infectious influenza virus. The test compounds were dissolved in phosphate-buffered saline containing 40% polyethylene glycol 400 and administered to mice through intraperitoneal injection at the indicated dosages twice daily for 5 days. Control mice received phosphate-buffered saline containing 40% polyethylene glycol 400 on the same schedule. Ten mice per test group were used throughout the studies. Four hours after the first dose of drug, mice were inoculated with influenza virus at 2X mouse LD₅₀. Mice were observed daily for 14 days for survival and body weight.

Molecular Modeling. All molecular modeling docking was performed on programs within the Schrodinger Suite. The influenza nucleoprotein (PDB code 2IQH) was refined by Prime (Schrodinger) and the A-chain monomer was applied as the target for molecular docking. A grid box was generated by using Glide (Schrodinger) to surround the tail-loop pocket of the desired compound. The compound was prepared by using LigPrep (Schrodinger) before molecular docking by using Glide. The protein-protein complex was obtained and refined further by using Prime and the VSGB solvation model. The OPLS_2005 force field was applied in all procedures.

■ ASSOCIATED CONTENT

Supporting Information

Supplementary tables detailing all compound structures and inhibition data for all viral strains tested, supplementary figures detailing molecular binding and analytical ultracentrifugation, methods for biological experiments and molecular modeling, and details on the synthesis and characterization of compounds are included in the supporting information. A document including the molecular formula strings for each analog is also available. The Supporting Information is available free of charge on the ACS Publications website.

■ AUTHOR INFORMATION

Corresponding Author

*Email: wong@scripps.edu,
chwong@gate.sinica.edu.tw. Tel: +886-2-27899929,
Fax: +886-2-27899927

Notes

The authors declare no conflict of interest.

■ ACKNOWLEDGMENT

This work was supported by the National Institutes of Health (AI130227-01A1), Academia Sinica [AS-SUMMIT-108] and Ministry of Science and Technology [MOST 108-3114-Y-001-002], and the Kwang Hua Foundation.

■ ABBREVIATIONS USED

CDI, carbonyldiimidazole; DCC, N,N'-dicyclohexylcarbodiimide; DCM, dichloromethane; DIPEA, N,N-diisopropylethylamine; DMF, dimethylformamide; DMSO, dimethylsulfoxide; EDC, 1-ethyl-3-(3-dimethylaminopropyl)carbodiimide hydrochloride; EtOAc, ethyl acetate; EtOH, ethanol; HATU, 1-[bis(dimethylamino)methylene]-1H-1,2,3-triazolo[4,5-b]pyridinium 3-oxid hexafluorophosphate; HBTU, 2-(1H-benzotriazol-1-yl)-1,1,3,3-tetramethyluronium hexafluorophosphate; HMDS, hexamethyldisilazane; HOBt, hydroxybenzotriazole; LAH, lithium aluminum hydride; LCMS, liquid chromatography mass spectrometry; MeOH, methanol; MW, microwave; NMM, N-methylmorpholine; NMR, nuclear magnetic resonance; TFA, trifluoroacetic acid; THF, tetrahydrofuran; TLC, thin layer chromatography; T3P, propylphosphonic anhydride; Xantphos, 4,5-bis(diphenylphosphino)-9,9-dimethylxanthene.

■ REFERENCES

- (1) World Health Organization: Influenza (Seasonal). World Health Organization Fact Sheet No. 211. **2014**.
- (2) McKimm-Breschkin, J. L. Influenza neuraminidase inhibitors: antiviral action and mechanisms of resistance. *Influenza Other Respir Viruses*. **2013**, 7, 25-36.
- (3) O'Hanlon, R.; Shaw, M. L. Baloxavir marboxil: the new influenza drug on the market. *Curr. Opin. Virol*. **2019**, 35, 14-18.

- (4) de Jong, M. D.; Tran, T. T.; Truong, H. K.; Vo, M. H.; Smith, G. J.; Nguyen, V. C.; Bach, V. C.; Phan, T. Q.; Do, Q. H.; Guan, Y.; Peiris, J. S.; Tran, T. H.; Farrar, J. Oseltamivir resistance during treatment of influenza A (H5N1) infection. *N. Engl. J. Med.* **2005**, *353*, 2667–2672.
- (5) Kiso, M.; Mitamura, K.; Sakai-Tagawa, Y.; Shiraishi, K.; Kawakami, C.; Kimura, K.; Hayden, F. G.; Sugaya, N.; Kawaoka, Y. Resistant influenza A viruses in children treated with oseltamivir: descriptive study. *The Lancet.* **2004**, *364*, 759–765.
- (6) Thorlund, K.; Awad, T.; Boivin, G.; Thabane, L. Systematic review of influenza resistance to the neuraminidase inhibitors. *BMC Infect. Dis.* **2011**, *11*, 134.
- (7) Nichol, K. L.; Treanor, J. J. Vaccines for seasonal and pandemic influenza. *J Infect Dis.* **2006**, *194*, Suppl 2, S111–118.
- (8) Elton, D.; Medcalf, E.; Bishop, K.; Digard, P. Oligomerization of the influenza virus nucleoprotein: identification of positive and negative sequence elements. *Virology.* **1999**, *260*, 190–200.
- (9) Mena, I.; Jambrina, E.; Albo, C.; Perales, B.; Ortin, J.; Arrese, M.; Vallejo, D.; Portela, A. Mutational analysis of influenza A virus nucleoprotein: identification of mutations that affect RNA replication. *J. Virol.* **1999**, *73*, 1186–1194.
- (10) Li, Z.; Watanabe, T.; Hatta, M.; Watanabe, S.; Nanbo, A.; Ozawa, M.; Kakugawa, S.; Shimojima, M.; Yamada, S.; Neumann, G.; Kawaoka, Y. Mutational analysis of conserved amino acids in the influenza A virus nucleoprotein. *J. Virol.* **2009**, *83*, 4153–4162.
- (11) Chan, W. H.; Ng, A. K.; Robb, N. C.; Lam, M. K.; Chan, P. K.; Au, S. W.; Wang, J. H.; Fodor, E.; Shaw, P. C. Functional analysis of the influenza virus H5N1 nucleoprotein tail loop reveals amino acids that are crucial for oligomerization and ribonucleoprotein activities. *J. Virol.* **2010**, *84*, 7337–7345.
- (12) Coloma, R.; Valpuesta, J. M.; Arranz, R.; Carrascosa, J. L.; Ortin, J.; Martin-Benito, J. The structure of a biologically active influenza virus ribonucleoprotein complex. *PLoS Pathog.* **2009**, *5*, e1000491.
- (13) Kukol, A.; Hughes, D. J. Large-scale analysis of influenza A virus nucleoprotein sequence conservation reveals potential drug-target sites. *Virol.* **2014**, *454–455*, 40–47.
- (14) Shu, L. L.; Bean, W. J.; Webster, R. G. Analysis of the evolution and variation of the human influenza A virus nucleoprotein gene from 1933 to 1990. *J. Virol.* **1993**, *67*, 2723–2729.
- (15) Ye, Q.; Krug, R. M.; Tao, Y. J. The mechanism by which influenza A virus nucleoprotein forms oligomers and binds RNA. *Nature.* **2006**, *444*, 1078–1082.
- (16) Ng, A. K.; Zhang, H.; Tan, K.; Li, Z.; Liu, J. H.; Chan, P. K.; Li, S. M.; Chan, W. Y.; Au, S. W.; Joachimiak, A.; Walz, T.; Wang, J. H.; Shaw, P. C. Structure of the influenza virus A H5N1 nucleoprotein: implications for RNA binding, oligomerization, and vaccine design. *FASEB J.* **2008**, *22*, 3638–3647.
- (17) Su, C. Y.; Cheng, T. J. R.; Lin, M. I.; Wang, S. Y.; Huang, W. I.; Lin-Chu, S. Y.; Chen, Y. H.; Wu, C. Y.; Lai, M. M. C.; Cheng, W. C.; Wu, Y. T.; Tsai, M. D.; Cheng, Y. S. E.; Wong, C. H. High throughput identification of compounds targeting influenza RNA-dependent RNA polymerase activity. *Proc. Natl. Acad. Sci. U.S.A.* **2010**, *107*, 19151–19156.
- (18) Kao, R. Y.; Yang, D.; Lau, L. S.; Tsui, W. H. W.; Hu, L. H.; Dai, J.; Chan, M. P.; Chan, C. M.; Wang, P.; Zheng, B. J.; Sun, J. A.; Huang, J. D.; Madar, J.; Chen, G. H.; Chen, H. L.; Guan, Y.; Yuen, K. Y. Identification of influenza A nucleoprotein as an antiviral target. *Nat. Biotechnol.* **2010**, *28*, 600–605.
- (19) Shen, Y. F.; Chen, Y. H.; Chu, S. Y.; Lin, M. I.; Hsu, H. T.; Wu, P. Y.; Wu, C. J.; Liu, H. W.; Lin, F. Y.; Lin, G.; Hsu, P. H.; Yang, A. S.; Cheng, Y. S.; Wu, Y. T.; Wong, C. H.; Tsai, M. D. E339...R416 salt bridge of nucleoprotein as a feasible target for influenza virus inhibitors. *Proc. Natl. Acad. Sci. U.S.A.* **2011**, *108*, 16515–16520.
- (20) Cheng, T. J.; Weinheimer, S.; Tarbet, E. B.; Jan, J. T.; Cheng, Y. S.; Shie, J. J.; Chen, C. L.; Chen, C. A.; Hsieh, W. C.; Huang, P. W.; Lin, W. H.; Wang, S. Y.; Fang, J. M.; Hu, O. Y.; Wong, C. H. Development of oseltamivir phosphonate congeners as anti-influenza agents. *J. Med. Chem.* **2012**, *55*, 8657–8670.
- (21) Liu, K. C.; Fang, J. M.; Jan, J. T.; Cheng, T. J.; Wang, S. Y.; Yang, S. T.; Cheng, Y. S.; Wong, C. H. Enhanced anti-influenza agents conjugated with anti-inflammatory activity. *J. Med. Chem.* **2012**, *55*, 8493–8501.
- (22) Chen, C. L.; Lin, T. C.; Wang, S. Y.; Shie, J. J.; Tsai, K. C.; Cheng, Y. S.; Jan, J. T.; Lin, C. J.; Fang, J. M.; Wong, C. H. Tamiphosphor monoesters as effective anti-influenza agents. *Eur. J. Med. Chem.* **2014**, *81*, 106–118.
- (23) Palmer, J. T.; Lunnis, C. J.; Offermann, D. A.; Axford, L. C.; Blair, M.; Mitchell, D.; Palmer, N.; Steele, C.; Atherall, J.; Watson, D.; Haydon, D.; Czaplowski,

L.; Davies, D.; Collins, I.; Tyndall, E. M.; Andrau, L.; Robert, G.; Pitt, W. Bacteria topoisomerase ii inhibiting 2-ethylcarbamoylamino-1,3-benzothiazol-5-yls. WO 2012045124 A1. April 12, **2012**.

(24) Woodring J.L.; Bachovchin K.A.; Brady K.G.; Gallerstein M.F.; Erath J.; Tanghe S.; Leed S.E.; Rodriguez A.; Mensa-Wilmot K.; Sciotti R.J.; Pollastri

M.P. Optimization of physicochemical properties for 4-Anilinoquinazoline inhibitors of trypanosome proliferation. *Eur J Med Chem.* **2017**, *141*, 446-459.

Table of Contents

